Morphology, Constraints, and Scaling of Frontal Sinuses in the Hartebeest, *Alcelaphus buselaphus* (Mammalia: Artiodactyla, Bovidae)

Andrew A. Farke*

Department of Anatomical Sciences, Stony Brook University, Stony Brook, New York 11794

ABSTRACT   The frontal sinuses of bovid mammals display a great deal of diversity, which has been attributed to both phylogenetic and functional influences. In-depth study of the hartebeest (*Alcelaphus buselaphus*), a large African antelope, reveals a number of previously undescribed details of frontal sinus morphology. In *A. buselaphus*, the frontal sinuses conform closely to the shape of the frontal bone, filling nearly the entire element. However, the horncores are never extensively pneumatized, contrasting with the condition seen in many other bovids. This evidence is inconsistent with the hypothesis that sinuses are opportunistic pneumatizing agents, suggesting that phylogenetic factors also play a role in determining sinus size. Both cranial sutures and neurovasculature appear to constrain the growth of sinuses in part. In turn, the sinus also affects the growth of the parietal; apparently this element is not truly pneumatized by the sinus in most cases, but the bone's shape changes under the influence of the sinus. Furthermore, the sinuses present relatively few struts when compared with the sinuses of some other bovids, such as *Ovis*. By adapting methods previously developed for measuring structural parameters of trabecular bone, it is possible to quantify certain aspects of sinus morphology. These include the number of bony struts within the sinus, the spacing of these struts, and the size of individual cavities within the sinus. Some differences in the number of struts are evident between subspecies. Similarly, significant differences occur in the relative number of struts between male and female *A. buselaphus*, which may be related to behavior. The volume of the sinus is strongly correlated with the size of the frontal, but less so with overall cranial size. This finding illustrates the importance of choosing variables carefully when comparing sinus sizes and growth between species. J. Morphol. 268:243–253, 2007.   © 2007 Wiley-Liss, Inc.

KEY WORDS: Alcelaphini; functional morphology; paranasal sinuses; pneumaticity

Pneumatic sinuses are one of the most infrequently described features in the vertebrate skull. These sinuses, which may originate from the nasal, tympanic, or pharyngeal regions, are internal structures that cannot be directly visualized without destructive methods or advanced imaging technology. Historically, cranial sinuses have been described only for a handful of representatives in each mammalian order by means of destructive sampling (e.g., Paulli, 1900). However, through the use of X-ray computed tomography (CT), pneumatic sinuses and associated internal features of the skull can be studied noninvasively. Most studies of sinus morphology, using CT imaging (and indeed, the historical bulk of all studies concerning sinuses), have focused on primates, and the majority of these papers have focused on the maxillary sinus (e.g., Koppe and Nagai, 1997; Rae and Koppe, 2003; Rossie, 2006). Nearly every paper published on sinuses calls for more comprehensive sampling of understudied clades, but few such descriptions exist. This limited taxonomic and anatomic scope hampers a more broad-scale understanding of the factors underlying sinus development.

Bovidae, the artiodactyl mammal clade containing sheep, goats, cattle and antelope, presents an ideal case study for sinus evolution. Recent phylogenetic hypotheses suggest that enlarged frontal sinuses evolved in this group at least three times (Vrba and Schaller, 2000). Some authors have proposed that frontal sinus morphology is adapted for certain modes of horn use, such as head butting (Schaffer and Reed, 1972). Alternatively, sinus morphology may track the morphology of the rest of the skull. For instance, if an animal evolves massive horns for head butting, the frontal bone must also be enlarged to support the horns. Because the frontal sinus is contained within the frontal bone, the sinus enlarges along with the bone itself. Thus, the sinus may not be a direct adaptation for head butting.

Regardless of the functional or evolutionary reasons for the presence of sinuses, any tests of such hypotheses are restricted by the limited data on frontal sinus morphology. Although the sinuses of

domesticated bovids have been well-described due to their veterinary significance (e.g., Nickel et al., 1978), domesticated taxa represent only a small subset of the total morphological diversity across bovids (over 120 species, ranging in total body mass from 3 to 1,200 kg). The frontal sinuses have been described and illustrated in some wild sheep and goats (Schaffer and Reed, 1972), but again this only represents a small sampling of the total morphological diversity within bovids.

Phylogenetic analyses of Bovidae often incorporate frontal sinus size and "complexity" as a character, without further elucidation or description in most cases (Vrba, 1979; Gentry, 1992; Vrba and Schaller, 2000). None of these analyses have discussed individual variation in the characters or provided quantitative support for the differentiation of character states, such as an extensive frontal sinus versus a restricted frontal sinus. A relationship between sex and sinus morphology has been suggested for some bovids (Schaffer and Reed, 1972), but this too has not been tested quantitatively. Thus, more complete descriptions are necessary to understand the functional and evolutionary significance of the frontal sinuses within bovids. By integrating these data with information on behavior and cranial morphology, a better understanding of the factors controlling the evolution of sinuses within the mammalian skull may be possible.

This study presents an in-depth description of the frontal sinuses in the hartebeest, *Alcelaphus buselaphus*. *Alcelaphus buselaphus* is a large African antelope, ranging in adult body mass from 116 to 228 kg. A number of subspecies are recognized, and they are differentiated on the basis of pelage, horn morphology, and other characteristics. Furthermore, *A. buselaphus* exhibits sexual dimorphism; the horns of females are generally more gracile than those of males. This dimorphism is associated with behavioral differences, in that males typically engage in horn-to-horn combat more frequently than do females. A number of other horn-related behaviors are also known, such as horning of the ground (Estes, 1991). Thus, *A. buselaphus* presents a spectrum of intraspecific, subspecific, and sexual variation, offering a chance to investigate potential relationships between sex, behavior, skull size, horn morphology, and sinus morphology. Only the frontal sinuses are considered here, because of their relevance to functional and phylogenetic hypotheses (see above), and because these sinuses are typically better preserved than other sinuses (for instance, the thin and delicate walls of the maxillary sinus are frequently broken in museum specimens). Although previous studies have investigated relationships between sinus volume and overall size of the skull or a segment of the skull, such as the facial skeleton (e.g., Rae and Koppe, 2000), none have examined specifically the relationship between a sinus and the bone within which it is contained.

Thus, three questions are specifically addressed in this study. First, what factor, if any, determines overall volume of the frontal sinuses? Second, how does the frontal sinus vary between subspecies of *A. buselaphus*? Finally, do male and female *A. buselaphus* differ in sinus morphology?

In addition to gross morphological descriptions for a single taxon, this study presents a novel application of methods for quantifying sinus dimensions. Previous studies, whether based on physical or digital measurement of the sinuses, have been restricted to simple cross-sectional area or volumetric measurements (e.g., Heyne and Schumacher, 1967; Koppe et al., 2000; Rae et al., 2003). However, sinuses are rarely simple chambers. In many animals, if not most, the sinuses are subdivided into a series of chambers by a number of bony struts (similar to the trabeculae seen in cancellous bone, only on a larger scale). A sinus with few struts, and thus few subchambers, is relatively simple, whereas a sinus with many struts and many subchambers is deemed complex (Schaffer and Reed, 1972). The degree of strutting is considered both phylogenetically and functionally significant (Schaffer and Reed, 1972; Vrba and Schaller, 2000), but strutting in sinuses has never been examined quantitatively. By adapting methods developed for quantifying trabecular bone architecture (Hildebrand and Rüegsegger, 1997), it is possible to count and measure the size distribution of a sinus's chambers and struts, in addition to basic volumetric measurements. This provides additional morphological variables, which can be tested, allowing a more thorough quantitative investigation of sinus function and evolution.

MATERIALS AND METHODS
Sample

Twenty four skulls of wild-shot *Alcelaphus buselaphus* were sampled from the collections of the Yale Peabody Museum of Natural History (YPM), New Haven, Connecticut (Table 1). Individuals were divided into five age classes by examining the relative degree of tooth wear on the upper molars: Stage 1, no molars erupted; Stage 2, only M^1 erupted; Stage 3, only M^2 erupted; Stage 4, M^3 erupted but barely worn; Stage 5, M^3 erupted and well-worn. For the purposes of this study, an animal was considered an adult at Stage 4. Individuals were assigned to subspecies and sex based on field data or horn morphology (when field data were absent). Because the horns are not fully developed in subadult individuals, some specimens could not be assigned to a species or sex. Two specimens of *A. b. lichtensteinii*, YPM 8952 and 9142, were sectioned along the midsagittal plane by a previous worker, allowing direct examination of the sinuses.

Measurements

Linear measurements. A suite of linear measurements was collected, using digital calipers (Appendix). These measurements were chosen to describe overall dimensions of the horns, frontal bone, and skull (exclusive of the horns and frontal).

Digital measurements. Specimens were scanned on a General Electric Lightspeed 16 CT scanner at Stony Brook University Hospital. Resolution and slice thickness varied by specimen, depending on skull size. Pixel size within a single slice ranged

Subspecies	Sex	YPM numbers	Age class
caama	M	7393	5
cokii	F	9156; 9582	5
		10267	4
	M	9127; 9131; 9185; 10473	5
		11519	?5[a]
jacksoni	M	9174; 9177; 11542	5
		10281	4
lichtensteinii	F	9205; 11534	5
	M	8952; 8955; 8968	5
		9106; 11535	4
	?	9137; 9142	3
		11543	2
ssp.	?	9190	3

[a]The age class of YPM 11519 is not certainly known, because the dentition is missing in this specimen. However, horn morphology and sutural fusion suggest that it belongs to age class 5.

between 0.49 and 0.98 mm, and slice thickness ranged between 1.25 and 2.50 mm.

3D Slicer (Open Source, 2006) was used to measure the volume of the frontal sinuses from the CT data as well as to create three-dimensional visualizations of the sinuses in relation to the skull. Because the horns of hartebeest are complexly shaped and vary in shape between subspecies, simple linear or curvilinear measurements are not sufficient to describe horn size in this sample. Thus, horn volume was calculated from the CT images for the keratinous horn sheath and bony horn core and used as a proxy for horn size.

Quantification of struts and cavities. To quantify the number of struts within the sinuses as well as describe the size of the cavities within the sinus, the frontal sinuses were measured, using techniques developed for quantitative structural analysis of trabecular bone. Trabecular bone, consisting of interconnected bony rods or plates surrounded by fluid-filled interstitial spaces, is analogous to the frontal sinuses of bovids, which consist of interconnected bony struts surrounded by air-filled cavities.

First, the bone was thresholded relative to the air in the sinus. Here, a modified version of the half-maximum height protocol used by Fajardo et al., (2002) (modified from a protocol developed by Spoor et al., 1993) was applied. Ten bone-air transitions for struts within the sinus were sampled on multiple slices across the dataset. Pixel values across the transition were measured, using ImageJ software (Rasband, 2006), and the mean of the highest and lowest values was used to define the transition for a single strut. The average of these midpoints from the ten samples was used as the global threshold for the bone-air interface across the entire scan.

In the program 3D Slicer (Open Source, 2006), the bone, sinus cavity, and air surrounding the specimen were segmented separately. The segmented slices were analyzed, using proprietary image analysis software designed for microCT data (Scanco, 2005). The software measures a series of parameters, but only a subset of them was used in this study. Indirectly-calculated parameters, determined using ratios between volume and surface area, assume a plate geometry for the struts and thus are inaccurate if the struts deviate from this assumption (Hildebrand et al., 1999). Instead, directly-calculated metrics (utilizing measurements of maximally-sized spheres that fit within a structure) were used here. Average cavity size and strut number (trabecular spacing, Tb.S*, and number, Tb.N*, respectively, of other authors; e.g., Hildebrand et al., 1999) were calculated to quantify the morphology of the struts within the sinus. Average cavity size, or strut spacing, measures the average diameter of the chambers within the sinus as determined by spherical packing. A related measurement, maximum cavity size, was also calculated. Strut thickness (trabecular thickness, Tb.Th* was not considered here, as the re-

solution of the scans was not considered sufficient to measure this parameter accurately in all specimens. Because the walls of the sinus (the roof of the frontal and the braincase) are not relevant to the metrics of sinus geometry studied here, these structures were excluded from calculations of strut number. The walls were included, however, in other calculations, because they would constrain the diameters of cavities within the sinus. A complete description of these methods is presented elsewhere (Hildebrand and Rüegsegger, 1997; Hildebrand et al., 1999).

To validate the computed measurements of strut number, struts were counted visually for all of the reconstructed sinuses in dorsal view. The septum separating the left and right frontal sinuses was considered one strut. Each strut originating from this septum and projecting medially was considered a separate strut, and so forth. Struts in other portions of the sinus (e.g., the caudal wall) were not counted, because they could not be distinguished consistently.

Data Analysis

To test the validity of the computed strut counts, a correlation matrix for a variety of measures related to the number of struts and number of subcavities within the sinuses was computed using Spearman's rho. Spearman's rho, rather than a parametric correlation coefficient, was chosen because a Kolmogorov–Smirnov test indicated that not all of the variables were distributed normally (Sokal and Rohlf, 1995). Analyzed measurements included adjusted visual strut counts (Measurement 34 in the Appendix), computed strut frequency (Measurement 25, both raw and corrected for sinus volume), and the sinus complexity index (SCI, Measurement 35). The SCI was created as an alternative metric describing the number of cavities within the sinus. This ratio is calculated as the average spherical diameter within the sinus (Measurement 24) over the cube root of sinus volume (Measurement 30). A sinus with many struts should have a smaller average chamber diameter than a sinus of equal size and similar shape with fewer struts, and thus the sinus with many struts should have a lower SCI. The results of the correlation analysis were used to select appropriate variables for subsequent analysis.

Volumetric measurements were transformed by a cube root prior to analysis. A proxy for skull size was determined by calculating the geometric mean of 15 cranial measurements (Measurement 27, Appendix). Use of a geometric mean mitigates any potential problems caused by relying on a single measurement (e.g., skull length) as a measurement of skull size. The measurements incorporated in the geometric mean excluded those related to horn or frontal size. Because the frontal is not a plate-like bone, a proxy for frontal size was determined by calculating the geometric mean of three measurements of the frontal (Measurement 29, Appendix). Ratios were calculated for relative sinus size, percent horncore pneumaticity, and percent of sinus contained within largest cavity (Measurements 31–33, Appendix). Visually estimated strut counts were divided by the cube root of sinus volume (in units of mm), to obtain a number that could be compared across individuals of various sizes. The geometric means and ratios were corrected for non-normality using a log transform (Sokal and Rohlf, 1995). The data were not transformed for nonparametric tests. Statistical analyses of the data were performed in SPSS (SPSS Inc., 2001), PAST (Hammer et al., 2006), Resampling Procedures (Howell, 2001) and BIOMstat (Applied Biostatistics Inc., 2002).

Several analyses were run on the data, to investigate a spectrum of questions. To explore what most closely determines sinus volume, a multiple linear regression was performed. Sinus volume was treated as the dependent variable, and skull size, frontal size, and horn size were treated as independent variables. Independent variables were added to the model using the "enter" protocol. The regression was run both for the entire sample ($n = 24$) and a subsample, including only adult males from all subspecies ($n = 15$), to control for age effects and sex. To explore individual
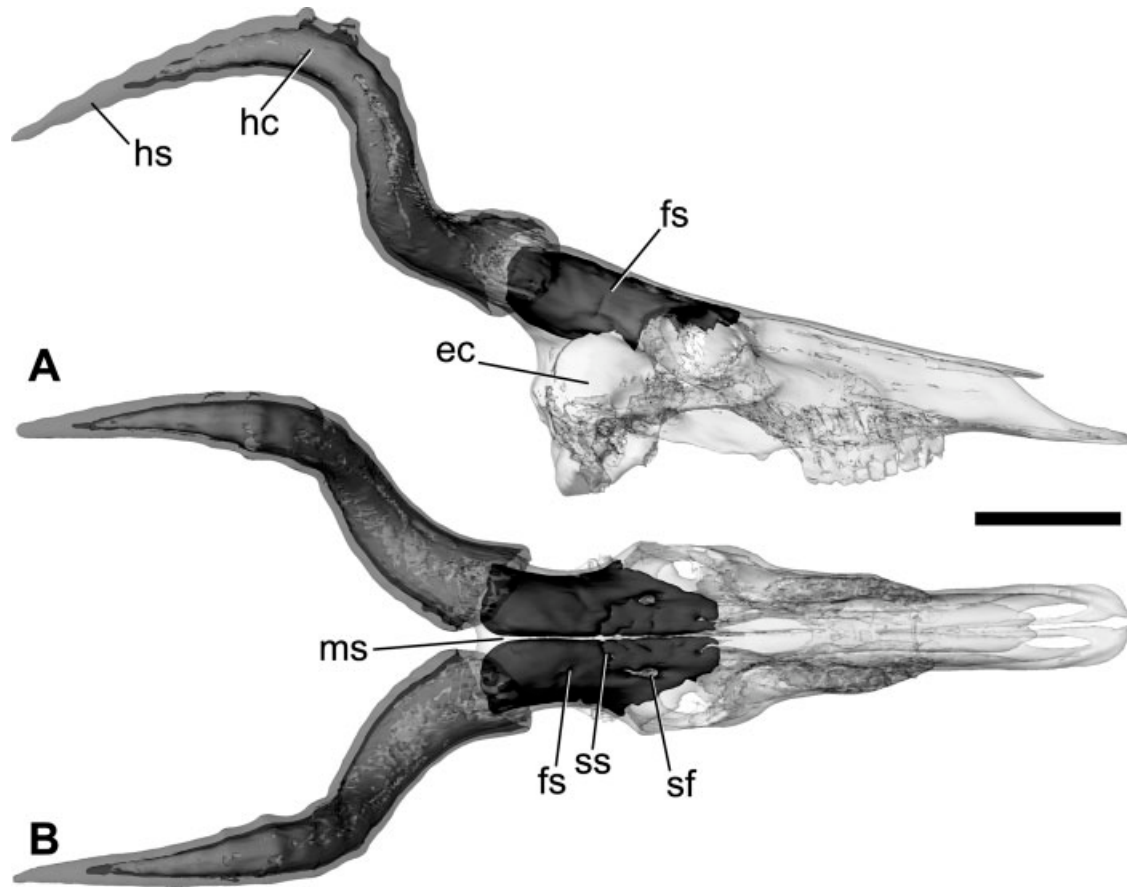
Fig. 1. *Alcelaphus buselaphus cokii* skull YPM 9131, reconstructed from CT scan data to show the position of the frontal sinuses relative to other cranial structures. **A**: Right lateral view. **B**: Dorsal view. ec, endocranial cavity; fs, frontal sinus; hc, horn core; hs, horn sheath; ms, midline strut; sf, supraorbital foramen; ss, supraorbital strut. Scale bar = 100 mm.

relationships between sinus volume, frontal size, and skull size, reduced major axes (RMA) regression was performed on all combinations of these three variables, for the entire sample and subsets, including adult males only and all individuals of *Alcelaphus buselaphus lichtensteinii* (the subspecies with the largest sample).

Interspecific differences in relative sinus volume, percent of sinus contained within largest cavity, horn pneumaticity, SCI, and visual strut counts were compared between adult male individuals of *Alcelaphus buselaphus cokii* ($n = 5$), *A. b. jacksoni* ($n = 4$), and *A. b. lichtensteinii* ($n = 5$). Females were excluded from this analysis, to avoid potential effects of sexual dimorphism. The measurements, grouped by species, were compared using T′ and Tukey–Kramer methods (Sokal and Rohlf, 1995). Differences in the same suite of variables were compared between adult male and female individuals of *A. b. cokii* (males, $n = 5$; females, $n = 3$), and *A. b. lichtensteinii* (males, $n = 5$; females, $n = 2$), using a randomization test to compare the means (due to the extremely small sample size for the females).

RESULTS
Anatomy of the Frontal Sinus

The gross morphology of the frontal sinus is remarkably conservative across the sample, irrespective of sex, subspecies, or age. In general, the extent of the frontal sinus conforms closely with the mor-

phology of the containing frontal bone (Fig. 1). The concave ventral aspect of the sinus appears to nestle the rostral portion of the endocranial cavity.

Virtually the entire extent of the frontal bone is pneumatized, from its contact with the nasal back to its suture with the parietal. Even the frontal portion of the orbital margin is fully pneumatized, out to the very edge (Fig. 1). A thick midline strut, coinciding with the interfrontal suture, separates the left and right frontal sinuses (Figs. 1 and 2). In all specimens, the supraorbital canal is at least partially enclosed by bone and surrounded by the cavities of the sinus. In all of the individuals, the supraorbital canal marks the rostral limit of a septum (here termed the supraorbital strut) that divides each frontal sinus into a medial and lateral portion. The strut runs caudomedially from the canal to the midline (Figs. 1B and 2). Beyond this, the number of struts varies between individuals, and even between the left and right sinuses. In general, the medial chamber displays more strutting than does the lateral chamber, and the rostral portion of the sinus displays more strutting than the caudal portion (Fig. 2).
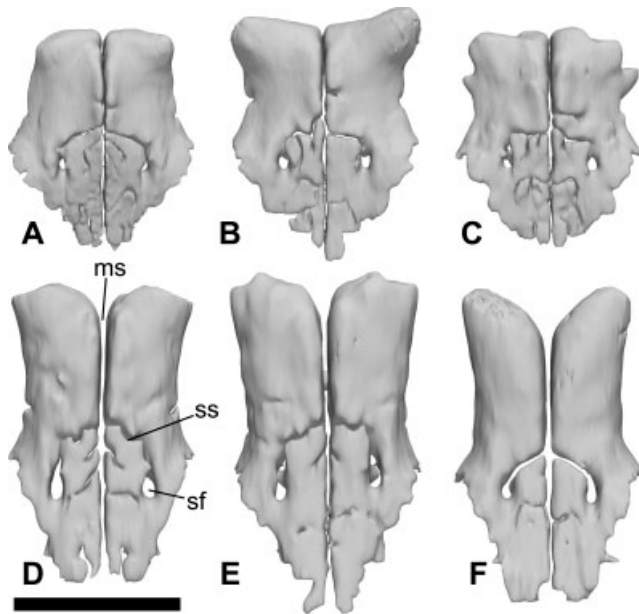
Fig. 2. Digital endocasts of frontal sinuses from *Alcelaphus buselaphus*. **A–C**: *A. b. lichtensteinii*. A: YPM 11543, subadult. B: YPM 9205, adult female. C: YPM 8955, adult male. **D**: *A. b. cokii*, YPM 9131, adult male. **E**: *A. b. jacksoni*, YPM 10281, adult male. **F**: *A. b. caama*, YPM 7393, adult male. ms, midline strut; sf, supraorbital foramen; ss, supraorbital strut. Scale bar = 100 mm.

In *Alcelaphus buselaphus caama*, *A. b. cokii*, and most *A. b. jacksoni*, the portion of the sinus caudal to the supraorbital canal is typically a simple, open chamber (Fig. 2D–F). In adult male *A. b. lichtensteinii* and some *A. b. jacksoni*, a series of struts divides the caudal wall of the frontal sinus within the base of the horn (Fig. 2C); they are typically more prominent in *A. b. lichtensteinii* than in *A. b. jacksoni*. Such struts were not observed in female and subadult specimens (Fig. 2A,B). One or two additional struts occasionally occur between the supraorbital strut and the caudal wall of the sinus.

None of the specimens shows significant pneumatization of the horncore (Table 2; contrasting with the condition seen in the closely-related alcelaphine *Damaliscus lunatus*; personal observation). At most, only the very base of the horn is pneumatized.

In at least some specimens, it appears that the parietal is also pneumatized by the frontal sinus, so that the parietal forms both the floor and roof of the caudal portion of the sinus. Reference to the sectioned skulls clarifies this morphology. In a subadult skull, YPM 9142, a scarf joint joins the frontal and parietal as they overlie the endocranium, forming the floor of the sinus (Fig. 3). The frontal rides over the top of the parietal (i.e., it is dorsal), continuing caudally over the parietal for about 25–30 mm. Caudally, the frontal portion of the joint becomes extremely thin, but it is still present. So, the sinus is not crossing sutural boundaries (even though it would appear to do so in an adult specimen or in a CT scan), and it is fully contained within the frontal, at least on the ventral floor of the sinus. The condition on the dorsal roof of the sinus is less clear. A similar veneer of frontal bone covers the parietal along the midline septum. In the sectioned adult skull, YPM 8952, the veneer is preserved only in one location laterally. This may be due to postmortem damage or resorption of the frontal veneer during life. Thus, even if the parietal isn't actually pneumatized (being separated from the frontal sinus by a thin sheet of bone at least in the subadult), it is effectively pneumatized.

A single exception to containment within the frontal and parietal is found in the specimen YPM 10281, *Alcelaphus buselaphus jacksoni*. In this individual, a portion of the frontal sinus enters the occipital bone. However, this "occipital sinus" is irregularly shaped and unilateral, strongly suggesting that it is anomalous.

Statistical Results

In the multiple regression analysis, including all specimens, only frontal size is a significant predictor of frontal sinus volume ($P < 0.001$, $R^2 = 0.783$). Similar results are achieved with other methods of variable selection (e.g., stepwise addition and backward subtraction), and nearly identical results are found when data were analyzed without the log transformation.

In the multiple regression analysis, including only males, both frontal size ($P < 0.010$) and horn size ($P < 0.019$; $R^2 = 0.865$) are selected as signifi-

TABLE 2. *Summary of selected cranial measurements from adult* Alcelaphus buselaphus *specimens*

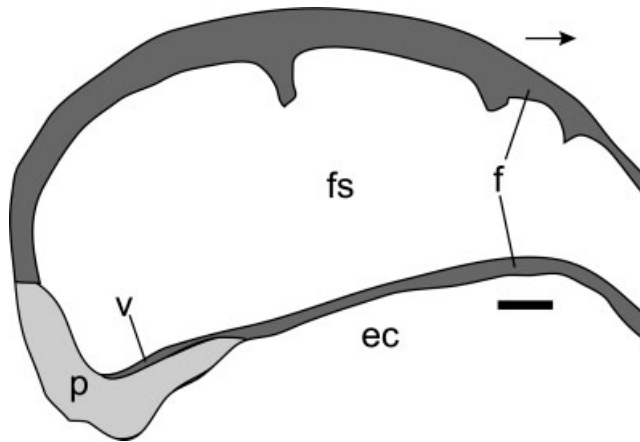| Subspecies	Sex	n	Skull length (mm)		Frontal sinus volume (ml)		Percent of horn pneumatized		Sinus complexity index	
			Mean	S.D.	Mean	S.D.	Mean	S.D.	Mean	S.D.
A. b. caama	M	1	395		385		5.3		0.45	
A. b. cokii	M	5	395	13	299	65	3.4	2.6	0.46	0.02
	F	3	403	30	223	107	2.5	1.6	0.40	0.01
A. b. jacksoni	M	4	407	17	513	48	4.3	2.0	0.47	0.01
A. b. lichtensteinii	M	5	430	23	491	71	0.8	0.20	0.34	0.02
	F	2	404	11	391	45	7.7	1.20	0.38	0.00

Fig. 3. Schematic parasagittal section through the frontal and frontal sinus in a subadult *Alcelaphus buselaphus lichtensteinii* skull, YPM 9142, showing the relationship between the frontal and parietal bones. ec, endocranial cavity; f, frontal; fs, frontal sinus; p, parietal; v, veneer of frontal bone. Arrow indicates the rostral direction on the specimen. Scale bar = 10 mm.

cant predictors of frontal sinus volume. Again, similar results are achieved with other methods of variable selection and without the log transformation.

The results of the individual RMA regressions are presented in Table 3 and Figure 4. For the analysis, including all specimens, only the regression of frontal size on skull size differs from isometry (slope = 1). All of the slopes overlap in their 95% confidence intervals, but the overlap is extremely small when comparing the regression of sinus volume on frontal size versus the regression of frontal size on skull size. For the regressions including only *Alcelaphus buselaphus lichtensteinii*, the regression of frontal sinus volume on frontal size is negatively allometric (slope < 1), but the regression of frontal size on skull size is positively allometric (slope > 1). None of the regressions for the adult males differ from isometry.

Only raw strut count (Measurement 26, Spearman's rho = 0.834, $P \ll 0.01$, $n = 23$) and SCI (Measurement 35, Spearman's rho = -0.529, $P < 0.01$, $n = 23$) are significantly correlated with adjusted visual strut count (Measurement 34). Neither the raw nor adjusted computed strut counts (Measurement 25) are correlated with raw or adjusted visual strut count ($-0.3 <$ Spearman's rho < 0.043; $P > 0.15$, $n = 23$). Based on these results, only SCI and adjusted visual strut count were used in subsequent analyses.

No significant differences occur in adjusted visual strut count between males of *Alcelaphus buselaphus cokii*, *A. b. jacksoni*, and *A. b. lichtensteinii*. However, male *A. b. lichtensteinii* have a significantly lower SCI ($P < 0.05$) than males of the other two species, which do not differ significantly from each other (see Table 2). Furthermore, male *A. b. lichtensteinii* pneumatizes a significantly smaller proportion of the horncore ($P < 0.05$) than either male *A. b. cokii* or male *A. b. jacksoni*, which do not differ from each other. A greater percentage of the sinus is contained within a single cavity for *A. b. cokii* than for the other two species. Relative to the skull, the frontal sinus of male *A. b. jacksoni* is larger than that of male *A. b. cokii* and male *A. b. lichtensteinii* ($P < 0.05$); males of the latter two species are not significantly different from each other.

Within *Alcelaphus buselaphus cokii*, males ($n = 4$) have a significantly higher SCI than females ($n = 3$, $P < 0.036$), but no significant differences exist between the sexes in percentage of horncore pneumatization, adjusted visual strut count, and relative sinus size. However, females are generally smaller in absolute sinus size (Table 2). Within *A. b. lichtensteinii*, females ($n = 2$) pneumatize a significantly greater percentage of the horncore than males ($n = 5$; $P < 0.05$), and males have a significantly lower SCI ($P < 0.04$); no other differences were observed. In an attempt to mitigate the effects of small sample size, the adult males ($n = 9$) and females ($n = 5$) from both previously considered subspecies were lumped for a single analysis; no significant differences were identified.

TABLE 3. *Comparisons of* RMA *regressions for* FSV, FS, *and* SS

Regression model	N	r^2	Slope	95% confidence limit on slope	Intercept
All specimens					
FSV on FS	24	0.75	.91	0.66–1.13	−0.28
FSV on SS	23	0.36	1.42	0.82–2.50	−1.35
FS on SS	23	0.46	1.57	1.08–2.47	−1.20
A. b. lichtensteinii only					
FSV on FS	10	0.73	.61	0.43–0.82	0.32
FSV on SS	10	0.69	1.15	0.65–1.51	−0.82
FS on SS	10	0.83	1.88	1.21–2.49	−1.86
Adult males only					
FSV on FS	15	0.79	1.10	0.84–1.36	−0.67
FSV on SS	14	0.62	1.26	0.89–1.76	−1.02
FS on SS	14	0.45	1.03	0.72–1.56	−0.079

FSV, frontal sinus volume; FS, frontal size; SS, skull size.
$P < 0.01$ for all values of r^2.
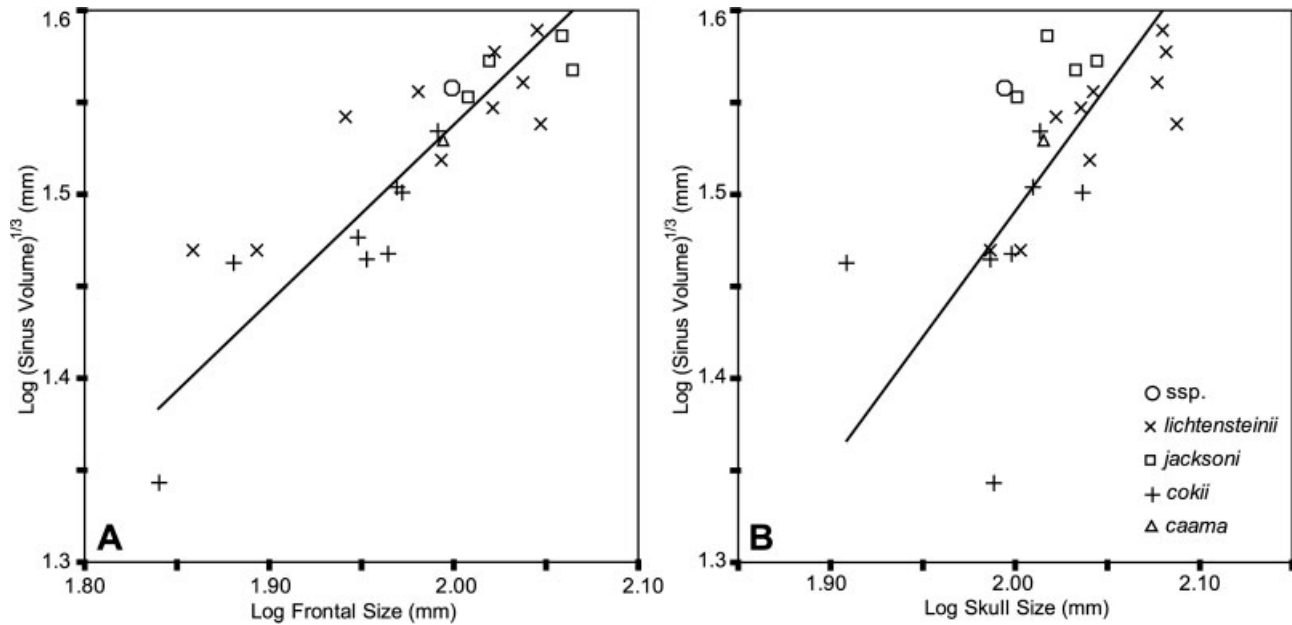n is reduced in some analyses due to missing data for certain specimens.

Fig. 4. Logarithmic plots of frontal sinus volume$^{1/3}$ versus **A**: log of frontal size and **B**: log of skull size, for the entire sample of hartebeest. Subspecies are indicated by the symbols explained in the lower right corner of B. The trend line was calculated using RMA regression; statistics for the regressions are given in Table 3.

DISCUSSION

The frontal sinus does not appear to cross sutural boundaries in most cases, either at the interfrontal suture or the frontoparietal suture. As described earlier, even where the parietal appears to be partially pneumatized, a thin veneer of bone from the frontal covers the parietal and presumably separates it from the soft tissue lining the sinus. These observations indicate that, at least in *Alcelaphus*, the cranial sutures may limit the expansion of sinuses. Furthermore, at least in the case where a veneer of frontal bone separated the sinus from the parietal, it also shows that the cranial sinuses may strongly influence the morphology of the surrounding, nonpneumatized bones. One interpretation of this condition is that the sinus, as it expands, pushes the frontal back over the parietal. This contrasts with the passive role typically suggested for the sinuses in cranial development (i.e., simply filling spaces otherwise occupied by "unnecessary" bone). Other studies have described cases of sinuses crossing sutural boundaries, such as the pneumatization of the zygomatic bone by the maxillary sinus in the platyrrhine primate *Alouatta caraya* (Koppe et al., 2005) or the hominoid primates *Pan* sp., *Pongo* sp., and *Gorilla* sp. (Rae and Koppe, 2000). Physical examination of both dry skulls and wet specimens is necessary to determine if the sinus truly crosses the suture in such cases. It is certainly possible that the zygomatico-maxillary suture already is obliterated by fusion in cases of zygomatic pneumatization by the maxillary sinus. In at least some birds, sinuses do not pneumatize across sutural boundaries until after they fuse (e.g., Bühler, 1981; Hogg, 1990). Because osteoclasts appear to be associated with sinus expansion (Smith et al., 2005a), but cranial sutures are a fibrocartilaginous tissue, it would be important to determine what types of cells are involved in sinus expansion at sutural boundaries. Additionally, developmental and structural differences between sutures in the splanchnocranium and sutures in the neurocranium (Rafferty and Herring, 1999) may also influence the pattern of expansion by the sinuses.

The neurovasculature of the supraorbital canal also appears to constrain sinus development. In all specimens studied, the bone of the supraorbital canal was mostly (if not completely) intact. Possibly, the bone is "needed" to support the nerves and blood vessels coursing through the canal. Yet, the developmental mechanism that would retain the wall of this bony canal is unclear.

Some aspects of sinus morphology are similar to the conditions seen in other taxa. For instance, a supraorbital strut with a configuration similar to that seen in *Alcelaphus buselaphus* also occurs in *Bos taurus* (Paulli, 1900). Further sampling is needed to determine the consistency of this feature. In particular, mapping the character across a phylogeny may establish if the supraorbital strut is a functional morphological feature or simply a consequence of sinus growth. Developmental studies also may provide additional insight into the development of this strut.

The results of the multiple regression models are consistent with the observation that the frontal sinus conforms closely to the boundaries of the frontal bone. Thus, it is not unexpected that frontal size is the major predictor of frontal sinus volume. In the multiple regressions, including only adult males, both frontal size and horn size were indicated as significant predictors of sinus volume. Again, the selection of frontal size is not surprising. An indirect relationship between horn size and sinus size is also to be expected, because the frontals support the horns. Thus, an increase in frontal size for support of larger horns results in a concomitant increase in frontal sinus volume. This is consistent with the hypothesis that sinus morphology is simply a byproduct of the surrounding cranial morphology. It is particularly noteworthy that skull size was not selected as a major predictor of sinus volume.

The results of the RMA regressions indicate some important patterns across the sample. First, as might be expected, the regressions vary depending on sample choice. This is illustrated by a comparison of the regressions of frontal sinus volume on frontal size (Table 3). When all individuals are lumped together, regardless of sex, subspecies, or age, sinus volume scales isometrically with frontal size. Similar results are seen for the sample including only adult males. This is expected, for the reasons listed above. However, sinus volume firmly scales with negative allometry relative to frontal size in the sample of *A. b. lichtensteinii*. In other words, frontal sinus volume does not increase as quickly as frontal size does. This may be due, at least in part, to the fact that juveniles (which are at the extreme low end of both frontal size and sinus volume) comprise nearly a third of the sample in this case. Thus, if the frontal sinus expands only after the frontal expands, negative allometry is expected. However, sample size is too small to explore the effects of removing juveniles in this case.

Furthermore, the correlations generally suggest a much tighter relationship between sinus volume and frontal size than between sinus volume and skull size (Table 3). These observations have important implications for other studies on sinus growth and size relative to the rest of the skull. Most studies of sinus growth have compared the volume of a sinus with a measurement or set of measurements representing overall cranial size, "facial volume," or another relatively generalized metric (Koppe and Nagai, 1997; Rae and Koppe, 2000). For instance, maxillary sinuses scale isometrically with "facial volume" in hominoid primates, but allometrically with basicranial length (Rae and Koppe, 2000). Given that the maxillary sinus is contained within the facial skeleton (specifically, the maxilla), it is entirely expected that the two metrics are isometrically related. Departures from this isometric relationship may indicate something truly interesting

about sinus function or development. Thus, overall cranial size is almost certainly inappropriate for examining trends in sinus size for most questions. Instead, it is recommended to examine sinus size in the context of its containing bones. For instance, in comparisons of the growth of the maxillary sinus, maxilla size (e.g., length, depth, and width measurements) would be preferable as a scaling variable, rather than overall facial size, snout length or basicranial length. Thus, such an analysis would be able to determine if differences in maxillary sinus volume are simply due to differences in maxilla size (or vice versa), rather than the relatively indirect relationships between sinus volume and overall cranial size. Although such differences have been observed qualitatively, none (aside from the present study) has investigated this quantitatively. In particular, this analytical approach is needed to resolve conflicting reports as to the influence of facial morphology on sinus morphology (Weidenreich, 1941; Koppe and Nagai, 1997). Here, departures of sinus volume relative to the volume of its containing bone are especially important. Yet, no previous studies have quantified this specifically.

The comparisons between subspecies did uncover some quantitative differences in certain morphological features, but interpreting these differences is problematic (particularly due to the small sample size). Visual comparison of sinus morphology (Fig. 2) suggests that *Alcelaphus buselaphus lichtensteinii* has qualitatively more complex sinuses than other subspecies. This is consistent with the lower SCI for this taxon. Most likely, the differences are attributable to variation in the shape and size of the frontal between the subspecies. In turn, as suggested by the multiple regression models, this is driven at least in part by horn morphology. Although behavior may play a role in some of this morphological disparity, no major differences in horn use have been reported between males of the hartebeest subspecies (Estes, 1991).

The results of the comparisons between genders are interesting, particularly when compared with the conditions in sheep and goats. In *Ovis canadensis*, *Ammotragus lervia*, and *Capra hircus hircus*, males and females have equally extensive cornual diverticula of the frontal sinus, but the sexes may differ greatly in the complexity of the frontal sinus (Schaffer and Reed, 1972). Struts within the sinus have been considered important for buttressing the sinus against loads applied to the horns (Schaffer and Reed, 1972). Because males engage in horn-to-horn combat more frequently than do females (Estes, 1991), it would be expected that males have more struts within their sinus. Although this was the case for *Alcelaphus buselaphus lichtensteinii* (at least for SCI), the opposite relationship was seen in *A. b. cokii*. Small sample size almost certainly affects these results. The hypothesis of an association between strut frequency and behavior should

be tested further, particularly for larger sample sizes. Furthermore, the mechanisms that might control strut formation should also be investigated. It would be of considerable interest to determine whether the strut patterns are determined genetically, epigenetically, or through a combination of both. Again, quantitative morphometric and ontogenetic studies are needed to investigate this in more detail.

The differences in the percentage of horncore pneumaticity between males and females of *Alcelaphus buselaphus lichtensteinii* contrasts with the lack of intersexual variation in this feature for *A. b. cokii* and caprines (Schaffer and Reed, 1972). A common statement about sinuses is that they remove mechanically unnecessary bone (e.g., Moore, 1981; Witmer, 1997). The condition in *A. b. lichtensteinii* is consistent with this hypothesis. If the horns of males experience loads of greater frequency and magnitude, it is expected that they would be more solid, as a solid horn offers greater strength than a hollow horn of equal linear dimensions. Thus, females should have more pneumaticity in their horns than males. However, this pattern does not extend to other hartebeest species, nor does it hold in sheep and goats. Indeed, if sinuses remove bone that is not needed for the structural support of the skull, it is quite puzzling that *A. buselaphus* horns (which presumably are subjected to relatively low magnitudes of force) are solid but *Ovis canadensis* horns (which presumably are subjected to relatively high magnitudes of force) are hollow. This suggests strongly that phylogenetic effects play an important role in dictating sinus morphology and size in bovids, in addition to epigenetic effects. Thus, the condition seen in the hartebeest is not entirely consistent with the idea of sinuses opportunistically removing "unnecessary" bone.

This study also illustrates the importance of validating specific measurements derived from CT data. Specifically, strut number (trabecular number of other authors) as calculated from the CT data did not correspond at all to the values derived from visual estimation, and thus was not a good measure of sinus complexity. Instead, the SCI was found to be a more reliable estimate of sinus complexity for the sample. The most likely reason for the poor correspondence between computed and visually-estimated strut counts is the relatively low number of struts contained within the hartebeest sinus. A tighter relationship may occur in taxa with a greater number of struts; such a pattern also should occur in trabecular bone. Although the SCI does not directly count the number of struts within the sinus, it is an adequate measure of complexity in the sample considered here. In particular, such computerized methods may be important for highly complex sinuses, where the number of struts cannot be easily counted visually. As confirmed by the correlation analysis, the SCI is inversely related to the number of struts within the sinus. As the number of struts in the sinus increases, the average size of the sinus's chambers should decrease.

The methods presented here for quantifying sinus morphology are applicable with little modification to nearly any structure for which three-dimensional data exist. Although such techniques have been used to quantify both trabecular bone and tooth root canal geometry (e.g., Hildebrand et al., 1999; Peters et al., 2001; Hübscher et al., 2003), this study is the first instance, in which the method has been applied to medical CT (versus micro CT) data. The possibilities for extensions of these methods are virtually limitless. Potential examples include the pneumatic chambers within bird and some nonavian dinosaur vertebrae, or the interconnected passageways of corals and sponges. These methods provide a quick and consistent way to describe quantitatively the complexity of these structures. This is an improvement on qualitative methods of describing these morphologies as simple or complex (e.g., Wedel, 2003). Furthermore, the present method could be used to quantify average thickness across irregularly-shaped structures, such as tooth enamel. This would represent an advance over the surface to volume ratio currently used to calculate average enamel thickness (Smith et al., 2005b), which can be affected greatly by shape.

CONCLUSIONS

The morphologies described here may be useful for phylogenetic analyses and for understanding evolutionary trends within alcelaphines. For instance, pneumatization of the parietal has not been reported previously, although it is a very constant feature across the sample of *Alcelaphus buselaphus*. Description of the sinuses within a larger cross section of bovids will prove useful in elucidating the relationships between the sinuses and the morphology of the rest of the skull. Larger sample sizes than those discussed here also will allow more detailed exploration of any trends.

Based on the sample of hartebeest, it appears that both sutures and neurovasculature play a role in guiding or limiting the growth of the sinuses within the skull. However, as evidenced by the influence of the frontal sinus on the parietal, the sinus may also influence the shape of a bone, which it does not directly pneumatize. Further work is needed to establish the factors that guide sinus development; in particular, a better understanding is needed of the interaction between the epithelium lining the sinus and the tissues surrounding or passing through the sinus. Additionally, the lack of pneumatization in the horncores of *Alcelaphus buselaphus* is somewhat perplexing, especially given the current paradigm of sinuses as opportunistic pneumatizers. Developmental and histological

work may prove fruitful for investigating these questions. Finite element modeling or other approaches may also be able to identify potential differences in the mechanical behavior of horns across taxa.

At least in the case of hartebeest, frontal sinus size is tightly linked to frontal size. A similar relationship is entirely expected for the maxillary and frontal sinuses of primates, a topic which may have considerable implications for interpretation of character evolution within this group. The statistical results presented here underscore the need for careful selection of scaling variables in studies comparing sinus size across and within taxa. Use of inappropriate metrics of comparison, such as basicranial length or facial volume, may obscure more relevant scaling relationships or correlations between sinuses and the bones containing them. Analyses comparing a suite of cranial measurements as well as different sinuses may well offer new insight into the broader question of the evolutionary forces driving sinus morphology.

ACKNOWLEDGMENTS

LITERATURE CITED

Applied Biostatistics Inc. 2002. BIOMstat [Statistical Analysis Software]. Version 3.30o. Port Jefferson, NY: Applied Biostatistics, Inc.

Bühler P. 1981. Functional anatomy of the avian jaw apparatus. In: King AS, McLelland J, editors. Form and Function in Birds Vol. 2. London: Academic Press. pp 439–468.

Estes RD. 1991. Behavior Guide to African Mammals. Berkeley: University of California Press. 611 p.

Fajardo RJ, Ryan TM, Kappelman J. 2002. Assessing the accuracy of high-resolution X-ray computed tomography of primate trabecular bone by comparisons with histological sections. Am J Phys Anthropol 118:1–10.

Gentry AW. 1992. The subfamilies and tribes of the family Bovidae. Mamm Rev 22:1–32.

Hammer Ø, Harper DAT, Ryan PD. 2006. PAST [Statistical Analysis Software]. Version 1.43. Oslo: University of Oslo.

Heyne K, Schumacher GH. 1967. Biometrische untersuchungen an den nebenhöhlen der nase von *Ovis aries*. Anat Anz 120:433–443.

Hildebrand T, Rüegsegger P. 1997. A new method for the model-independent assessment of thickness in three-dimensional images. J Microsc 185:67–75.

Hildebrand T, Laib A, Müller R, Dequeker J, Rüegsegger P. 1999. Direct three-dimensional morphometric analysis of human cancellous bone: Microstructural data from spine, femur, iliac crest, and calcaneus. J Bone Miner Res 14:1167–1174.

Hogg DA. 1990. The development of pneumatisation in the skull of the domestic fowl (*Gallus gallus domesticus*). J Anat 169:139–151.

Howell DC. 2001. Resampling Procedures [Statistical Analysis Software]. Version 1.3. Burlington: University of Vermont.

Hübscher W, Barbakow F, Peters OA. 2003. Root-canal preparation with FlexMaster: Canal shapes analysed by micro-computed tomography. Int Endod J 36:740–747.

Koppe T, Nagai H. 1997. Growth pattern of the maxillary sinus in the Japanese macaque (*Macaca fuscata*): Reflections on the structural role of the paranasal sinuses. J Anat 190:533–544.

Koppe T, Klauke T, Lee S, Schumacher G-H. 2000. Growth pattern of the maxillary sinus in the miniature pig (*Sus scrofa*). Cells Tissues Organs 167:58–67.

Koppe T, Moormann T, Wallner CP, Rohrer-Ertl O. 2005. Extensive enlargement of the maxillary sinus in *Alouatta caraya* (Mammalia, Primates, Cebidae): An allometric approach to skull pneumatization in Atelinae. J Morphol 263:238–246.

Moore WJ. 1981. The mammalian skull. Cambridge: Cambridge University Press. 369 p.

Nickel R, Schummer A, Seiferle E, Sack WO. 1978. The viscera of the domestic mammals. New York: Springer-Verlag. 401 p.

Open Source. 2006. 3D Slicer [Image Analysis Software]. Version 2.6-opt. Boston: Brigham and Women's Hospital.

Paulli S. 1900. Über die pneumaticität des schädels bei den säugerthieren. Eine morphologische studie. II. Über die morphologie des siebbeins und die der pneumaticität bei den ungulaten und probosciden. Gegenbaurs Morphol Jahrb 28:179–251.

Peters OA, Laib A, Göhring TN, Barbakow F. 2001. Changes in root canal geometry after preparation assessed by high-resolution computed tomography. J Endod 27:1–6.

Rae TC, Koppe T. 2000. Isometric scaling of maxillary sinus volume in hominoids. J Hum Evol 38:411–423.

Rae TC, Koppe T. 2003. The term "lateral recess" and craniofacial pneumatization in Old World Monkeys (Mammalia, Primates, Cercopithecoidea). J Morphol 258:193–199.

Rae TC, Hill RA, Hamada Y, Koppe T. 2003. Clinal variation of maxillary sinus volume in Japanese macaques (*Macaca fuscata*). Am J Primatol 59:153–158.

Rafferty KL, Herring SW. 1999. Craniofacial sutures: Morphology, growth, and in vivo masticatory strains. J Morphol 242:167–179.

Rasband W. 2006. ImageJ [Image Analysis Software]. Version 1.34s. Bethesda, MD: U.S. National Institutes of Health.

Rossie JB. 2006. Ontogeny and homology of the paranasal sinuses in Platyrrhini (Mammalia: Primates). J Morphol 267:1–40.

Scanco. 2005. Image Processing Language [CT Scan Analysis Software]. Version 4.30a. Zürich: Scanco Medical AG.

Schaffer WM, Reed CA. 1972. The co-evolution of social behavior and cranial morphology in sheep and goats (Bovidae, Caprini). Fieldiana 61:1–88.

Smith TD, Rossie JB, Cooper GM, Mooney MP, Siegel MI. 2005a. Secondary pneumatization of the maxillary sinus in callitrichid primates: Insights from immunohistochemistry and bone cell distribution. Anat Rec A 285:677–689.

Smith TM, Olejniczak AJ, Martin LB, Reid DJ. 2005b. Variation in hominoid molar enamel thickness. J Hum Evol 48:575–592.

Sokal RR, Rohlf FJ. 1995. Biometry. New York: W.H. Freeman. 887 p.

Spoor CF, Zonneveld FW, Macho GA. 1993. Linear measurements of cortical bone and dental enamel by computed tomography: Applications and problems. Am J Phys Anthropol 91:469–484.

SPSS Inc. 2001. SPSS [Statistical Analysis Software]. Version 11. Chicago: SPSS.

Vrba ES. 1979. Phylogenetic analysis and classification of fossil and recent Alcelaphini Mammalia: Bovidae. Biol J Linn Soc 11:207–228.

Vrba ES, Schaller GB. 2000. Phylogeny of Bovidae (Mammalia) based on behavior, glands and skull morphology. In: Vrba ES, Schaller GB, editors. Antelopes, deer, and relatives: Fossil record, behavioral ecology, systematics, and conservation. New Haven, CT: Yale University Press. pp 203–222.

Wedel MJ. 2003. The evolution of vertebral pneumaticity in sauropod dinosaurs. J Vert Paleont 23:344–357.

Weidenreich F. 1941. The brain and its role in the phylogenetic transformation of the human skull. Trans Am Philos Soc 31:320–442.

Witmer LM. 1997. The evolution of the antorbital cavity of archosaurs: A study in soft-tissue reconstruction in the fossil record with an analysis of the function of pneumaticity. Soc Vert Paleo Mem 3:1–73.

APPENDIX: MEASUREMENTS
General Skull Measurements

1. Greatest length of nasals
2. Greatest width across maxillary tuberosities
3. Minimum distance between the rostral ends of the orbit
4. Minimum distance between supratemporal lines
5. Greatest breadth across external surface of braincase
6. Greatest breadth across occipitals
7. Greatest distance between lateral edges of occipital condyles
8. Greatest distance between lateral edges of paroccipital processes
9. Mediolateral diameter of foramen magnum
10. Greatest length of maxillary tooth row
11. Greatest mediolateral breadth across maxillary tooth rows
12. Greatest length of skull, from caudal end of occipital condyles to rostral limit of premaxillae
13. Length from caudal limit of nasals to rostral limit of premaxillae

14. Rostro-caudal diameter of orbit
15. Distance from dorsal border of foramen magnum to caudal limit of nasals

Horn Measurements

16. Volume of horncore*
17. Volume of horn sheath*

Frontal Measurements

18. Frontal length, from caudal limit of frontal pedicle to point between supraorbital foramina
19. Greatest width between lateral surfaces of base of horncores
20. Greatest thickness of frontal at the midline*

Sinus Measurements

21. Volume of frontal sinuses*
22. Volume of frontal sinus contained within the horncore*
23. Maximum spherical diameter of cavities within the sinus*
24. Average spherical diameter of chambers within the sinus (=Tb.Sp*)[1]
25. Computed strut frequency (n/mm, = Tb.N*)[1]
26. Visual strut count*

Derived Measurements

27. Skull size (geometric mean of Measurements 1–15)
28. Total volume of horn (sum of Measurements 16 and 17)
29. Frontal size (geometric mean of Measurements 18–20)
30. Frontal sinus size (cube root of 21)
31. Percent of horncore pneumatized by frontal sinus (22/16)
32. Relative sinus size (30/27)
33. Percent of sinus contained within largest cavity (volume of largest sphere as calculated from 23/21)
34. Adjusted visual strut count (26/30)
35. Sinus complexity index or SCI (24/30)

---

[1]Indicates measurements measured directly from CT data.